Pharmaceutical Research, Vol. 23, No. 5, May 2006 (© 2006)
DOI: 10.1007/s11095-006-9902-8

Research Paper

In Vitro Studies of Intestinal Permeability and Hepatic and Intestinal Metabolism of 8-Prenylnaringenin, a Potent Phytoestrogen from Hops (*Humulus lupulus* L.)

Dejan Nikolic,[1] Yongmei Li,[1] Lucas R. Chadwick,[1] and Richard B. van Breemen[1,2,]

Received September 3, 2005; accepted January 5, 2006

Purpose. The absorption potential and metabolism of 8-prenylnaringenin (8-PN) from hops (*Humulus lupulus* L.) were investigated. 8-PN is a potent estrogen with the potential to be used for the relief of menopausal symptoms in women.
Methods. Monolayers of the human intestinal epithelial cancer cell line Caco-2 and human hepatocytes were incubated with 8-PN to model its intestinal absorption and hepatic metabolism, respectively.
Results. The apparent permeability coefficients for 8-PN in the apical-to-basolateral and basolateral-to-apical directions of a Caco-2 monolayer were $5.2 \pm 0.7 \times 10^{-5}$ and $4.9 \pm 0.5 \times 10^{-5}$ cm/s, respectively, indicating good intestinal absorption via passive diffusion. Both glucuronide and sulfate conjugates of 8-PN were detected in the Caco-2 cell incubations. The 4′-*O*-glucuronide was the predominant Caco-2 cell metabolite, followed by 7-*O*-sulfate and 4′-*O*-sulfate. Both phase I and phase II metabolites of 8-PN were formed by human hepatocytes. The 7-*O*-glucuronide was the most abundant hepatocyte metabolite, and no sulfate conjugates were detected. Incubations with various cDNA-expressed UDP-glucuronosyltransferases indicated that the isozymes UGT1A1, UGT1A6, UGT1A8, and UGT1A9 were responsible for glucuronidation of 8-PN.
Conclusions. Although orally administered 8-PN should be readily absorbed from the intestine, its bioavailability should be reduced significantly by intestinal and hepatic metabolism.

KEY WORDS: Caco-2 cells; hops; liquid chromatography–mass spectrometry (LC–MS); metabolism; natural products; 8-prenylnaringenin.

INTRODUCTION

The female flowers of hops (*Humulus lupulus* L.) are used in the brewing industry as a flavoring agent for beer. Recently, there has been interest in the potential estrogenic activities of hop extracts. Based on anecdotal reports of menstrual disturbances among women who pick hops in Germany, menopausal women sometimes take hops baths to seek relief from hot flashes (1). In addition, hops extracts have become major constituents of an increasing number of commercial preparations marketed for breast enhancement (2).

Among the possible active constituents, the flavonoid 8-prenylnaringenin (8-PN; see structure in Fig. 1) has attracted the most attention. 8-PN belongs to the group of prenylated flavanones, which includes isoxanthohumol, 6-prenylnaringenin, and a number of diprenylated analogs (3). Various *in vitro* studies have identified 8-PN as one of the most potent estrogens in hops with a potency equal to or greater than other established plant estrogens such as genistein or coumestrol (1,4,5). Milligan *et al.* (6) showed that 8-PN is estrogenic in rats *in vivo*, although its activity seemed to be much weaker than that of estradiol.

Few data exist in the literature concerning the metabolism or bioavailability of 8-PN or other prenylated flavonoids. Yilmazer *et al.* (7,8) studied rat liver microsomal metabolism of xanthohumol and identified four phase I metabolites and two phase II glucuronides. We have identified several phase I metabolites of 8-PN formed by human liver microsomes (9). In the present study, we investigated the intestinal permeability and metabolism of 8-PN using human Caco-2 cell monolayers as a model system for intestinal absorption and metabolism. In addition, incubation of 8-PN with human hepatocytes was used as a model for liver metabolism.

[1] Department of Medicinal Chemistry and Pharmacognosy, UIC/NIH Center for Botanical Dietary Supplements Research, College of Pharmacy, University of Illinois at Chicago, 833 S. Wood Street, Chicago, Illinois 60612-7231, USA.
[2] To whom correspondence should be addressed. (e-mail: breemen@uic.edu)

ABBREVIATIONS: ABCC2 (MRP2), multidrug-resistance-associated protein-2; AP, apical; BL, basolateral; CID, collision-induced dissociation; CYP, cytochrome P450; FWHM, full width at half maximum; HPLC, high-performance liquid chromatography; LC–MS, liquid chromatography–mass spectrometry; LC–MS–MS, liquid chromatography tandem mass spectrometry; TEER, transepithelial electrical resistance; UGT, uridine diphosphoglucuronosyltransferase; 8-PN, 8-prenylnaringenin.

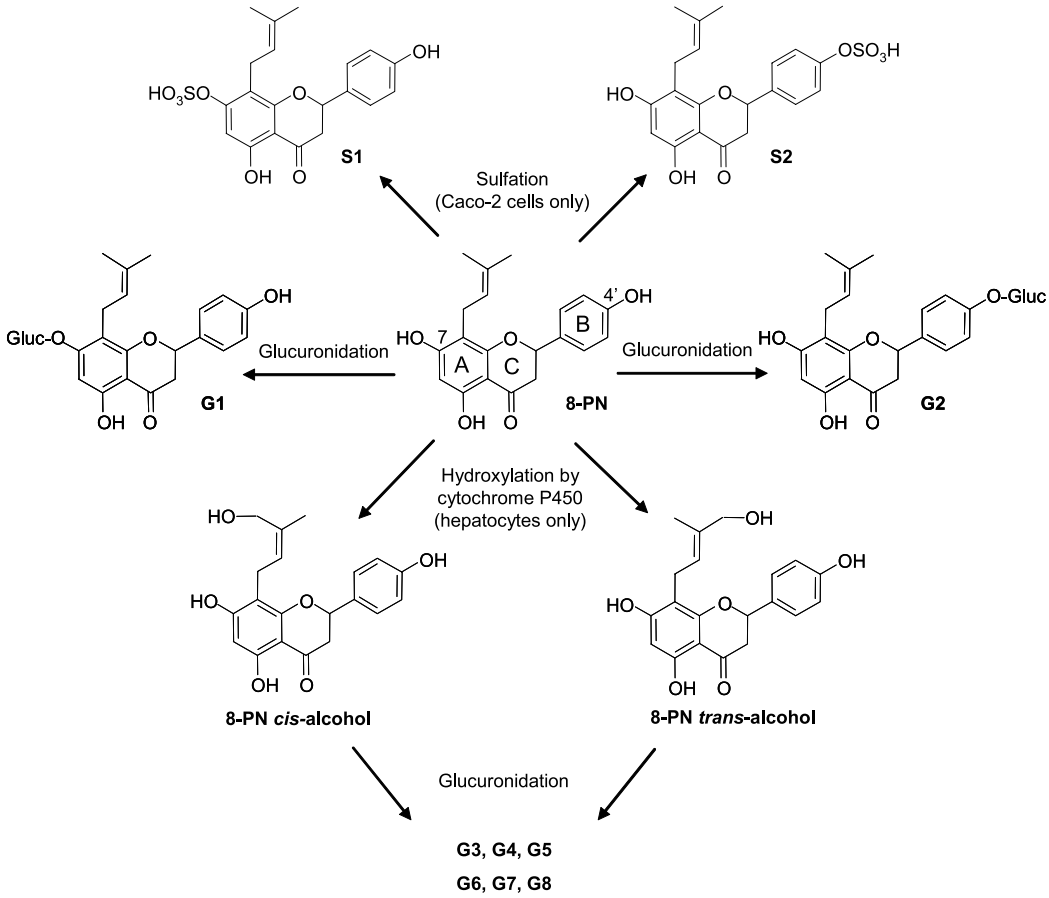

Fig. 1. Structures of metabolites and pathways of *in vitro* phase II conjugation of 8-PN by Caco-2 cell monolayers and human hepatocytes. Note that S1 and S2 are sulfate conjugates and that G1–G8 are glucuronides.

Together, these two models provided important predictive information regarding the oral bioavailability of 8-PN.

MATERIALS AND METHODS

Chemicals

Racemic 8-PN was isolated from a methanolic extract of spent Nugget hops (*Humulus lupulus* cv. Nugget, plant material previously extracted with supercritical carbon dioxide) and purified by semipreparative high-performance liquid chromatography (HPLC). Purity was determined to be >98% based on HPLC and liquid chromatography–mass spectrometry (LC–MS) analyses. Uridine diphosphoglucuronic acid, mannitol, propranolol, naringenin, β-glucuronidase (type B-10 from bovine liver), and sulfatase (type VI, from *Aerobacter aerogenes*, partially purified) were purchased from Sigma-Aldrich (St. Louis, MO, USA). MK571 was purchased from Cayman Chemical (Ann Arbor, MI, USA). All organic solvents were HPLC-grade and were purchased from Fisher Scientific (Fair Lawn, NY, USA).

The Caco-2 cell line (originating from a human colorectal carcinoma), Eagle's minimum essential medium, and fetal bovine serum were purchased from the American Type Culture Collection (Rockville, MD, USA). Trypsin–EDTA (0.25%), Hank's balanced salt solution (HBSS), penicillin, and streptomycin were purchased from Life Technology (Grand Island, NY, USA). Six-well cell culture plates with polycarbonate inserts (24.4 mm in diameter, 4.71 cm^2 surface area, and 3.0 μm pore size) were purchased from Corning Costar (Cambridge, MA, USA). The Millicell-ERS instrument used for measuring the transepithelial electrical resistance (TEER) of the Caco-2 cell monolayers was obtained from Millipore (Bedford, MA, USA). Cryopreserved human hepatocytes were purchased from *In Vitro* Technologies (Baltimore, MD, USA) and were handled according to the supplier's instructions. cDNA-expressed uridine diphosphoglucuronosyltransferases (UGTs), prepared from baculovirus-infected insect cells (SUPERSOMES™), were purchased from Gentest (Woburn, MA, USA).

Cell Culture

Caco-2 cells were cultured at 37°C in an atmosphere of 5% CO_2 and 90% relative humidity in Eagle's minimum essential medium with 10% fetal bovine serum, 100 U/mL penicillin, and 100 μg/mL streptomycin. Confluent monolayers were subcultured every 7 days by treatment with 0.25% trypsin containing EDTA. For transport and metabolism studies, Caco-2 cells (passage numbers 20–35) were seeded onto polycarbonate membranes at a density of 2×10^5 cells per insert and grown to late confluence (15–21 days).

The culture medium was changed every other day after seeding. The integrity of the monolayers of the differentiated Caco-2 cells was monitored by measuring the TEER value, and only monolayers with values >300 $\Omega \cdot cm^2$ were used.

Measurement of Apparent Permeability Coefficients

After the complete culture medium was removed from both the apical (AP) and basolateral (BL) chambers, the monolayers were washed three times and then preincubated with HBSS at pH 7.4 for 30 min at 37°C on a shaker bath at 50 rpm. 8-PN was added to either the apical chambers (for AP → BL permeability measurements) or the basolateral chambers (for BL → AP studies) at an initial concentration of 50 μM in HBSS. The concentration of 50 μM was selected because it is a biologically relevant concentration of 8-PN that might occur in the intestinal lumen following oral administration of 8-PN or hops preparations enriched in 8-PN. As a marker of paracellular transport, mannitol (50 μM final concentration) was added to each apical chamber. In separate Caco-2 control experiments, propranolol was added to the apical chamber at 10 μM and assayed as described above for 8-PN as an example of a high-permeability compound. The volumes of the solutions in the apical and basolateral chambers were 1.5 and 2.6 mL, respectively.

At the time points 5, 10, 20, 40, or 60 min, solutions in the recipient compartments of the incubations described above were removed and replaced with fresh medium. The samples were stored at −20°C until analysis for 8-PN using LC–MS. These samples were analyzed for 8-PN, mannitol, and, in some experiments, propranolol. The apparent permeability coefficients (P_{app}) expressed in centimeters per second were calculated using the following equation: $P_{app} = V_R \times dC/dt \times 1/AC_0$. V_R is the volume of the recipient compartment (2.6 and 1.5 mL for basolateral and apical compartments, respectively); dC/dt is the slope of the cumulative concentration (micromolar) of 8-PN in the recipient chamber over time (seconds); A is the membrane surface area (4.71 cm^2); and C_0 is the initial concentration of 8-PN in the donor chamber (micromolar). The apparent permeability coefficients were obtained under "sink conditions," i.e., less than 10% transported, to minimize diffusion of the solute back from the receiving to the donor compartment. All experiments were carried out in triplicate.

During the Caco-2 permeability studies, the TEER values of the Caco-2 cell monolayers measured before and after the 1-h incubations were determined to be identical at 554 ± 12 and 542 ± 14 $\Omega \cdot cm^2$, respectively. As a low-permeability control, the apparent permeability coefficient of mannitol was measured in the apical-to-basolateral direction and was acceptably low at 0.32 (±0.02) × 10^{-6} cm/s (N = 3). In addition, the apparent permeability coefficient of the high-permeability standard propranolol was determined in the apical-to-basolateral direction and was appropriately high at 5.4 (±0.4) × 10^{-5} cm/s (N = 3). These experiments verified the integrity of the Caco-2 cell monolayers and helped calibrate the assay.

Caco-2 Cell Metabolism of 8-PN

A 1.5-mL aliquot of a 50-μM 8-PN solution (in HBSS) was added to either the apical or basolateral chambers of the Caco-2 cell monolayers. After 4 h of incubation, both apical and basolateral solutions were collected for LC–MS analysis of 8-PN and its metabolites. To determine the possible role of ABCC2 (MRP2) in the transport of 8-PN phase II conjugates, 8-PN was incubated with Caco-2 cells for 4 h exactly as described above except that the ABCC2 (MRP2) inhibitor MK571 (50 μM) was included to both the apical and basolateral chambers. These experiments were carried out in duplicate. The chemical stability of 8-PN in HBSS at 37°C was examined under the same conditions as in the metabolism study but without the Caco-2 cell monolayers. The TEER values of the Caco-2 cell monolayers were measured before and after the 4-h incubations to ensure monolayer integrity.

Metabolism of 8-PN by Human Hepatocytes

Cryopreserved hepatocytes were thawed according to the supplier's instructions, and approximately 1 × 10^6 cells in a 1-mL suspension were incubated with 8-PN (10-μL aliquot of a 5 mM solution in dimethyl sulfoxide) per well of a 12-well plate. Control experiments were identical except for the substitution with heat-inactivated hepatocytes. The plate was placed in an incubator at 37°C with 5% CO_2 and 90% relative humidity and gently shaken at 50 rpm for 4 h. Incubations were terminated by the addition of 3 mL of ice-cold methanol. The cell suspensions were centrifuged, and aliquots of the supernatants were analyzed using LC–MS and LC–MS–MS.

Glucuronidation by cDNA-Expressed UDP-Glucuronosyltransferases

Incubations with human recombinant UGT1A1, UGT1A6, UGT1A8, UGT1A9, UGT1A10, and UGT2B7 were carried out according to the protocol recommended by the supplier (Gentest) with the modifications of Fisher *et al.* (10). Briefly, 0.04 mg of the protein preparation was mixed with 2 μg alamethicin and 148 μL of 50 mM phosphate buffer (pH 7.4) and placed on ice for 15 min. Next, magnesium chloride (10 mM final concentration) and 8-PN (50 μM final concentration, added in 2 μl of methanol) were added, and the mixture was preincubated for 3 min at 37°C. Reactions were initiated by adding uridine diphosphoglucuronic acid (2 mM final concentration in a total volume of 0.2 mL), and incubations were carried out for 30 min. The reactions were terminated by the addition of 100 μL of acetonitrile/acetic acid (94:6, v/v), and each sample was centrifuged at 10,000 × g for 3 min. Finally, 10-μL aliquots of each supernatant were analyzed using LC–MS or LC–MS–MS.

LC–UV–MS and LC–MS–MS

Mass spectrometric analyses were carried out using a Waters (Milford, MA, USA) 2690 HPLC system interfaced to a Micromass (Manchester, UK) Q-TOF-2 hybrid quadrupole-time-of-flight mass spectrometer equipped with electrospray ionization. HPLC separations of 8-PN and its metabolites were carried out using a YMC (Wilmington, NC, USA) AQ 2.1 × 250 or 2.1 × 150 mm C_{18} column with a binary gradient solvent system consisting of 0.05% acetic acid in water (solvent A) and methanol (solvent B). The gradient program

consisted of 45% B for 10 min, a linear gradient from 45 to 68% B over 35 min, 68% B for another 5 min, a linear gradient from 68 to 90% B over the next 10 min, 90% B for 10 min, and finally returning to 45% B in 2 min. The flow rate was 0.2 mL/min.

Although negative ion electrospray provided the greatest signal-to-noise for metabolites of 8-PN, positive ion electrospray tandem mass spectrometry was also used to obtain complementary structural information for the metabolites. For most measurements, mass spectra were obtained at a resolving power of 5000 full width at half maximum (FWHM) at *m/z* 500. However, the resolving power was increased to 8000 FWHM at *m/z* 500 for exact mass measurements. Polyethylene glycol was used for calibration, and raffinose ($[M\text{-}H]^-$, *m/z* 503.1612) was added postcolumn as a lock mass for exact mass measurements. Data were acquired from *m/z* 250 to 900. Product ion tandem mass spectra were acquired using collision-induced dissociation (CID) with argon at a collision energy of 25 eV. UV spectra were obtained during LC–UV–MS over the range 190–370 nm using a photodiode array absorbance detector.

Propranolol and mannitol concentrations in the basolateral chambers were determined using an Agilent (Palo Alto, CA, USA) G1946A single quadrupole mass spectrometer with an 1100 HPLC system. Positive ion electrospray was used with selected ion monitoring to measure the protonated molecule of propranolol at *m/z* 260 and the protonated internal standard acebutolol at *m/z* 337. The internal standard was added immediately before LC–MS analysis to control for variations in sample handling and LC–MS response. HPLC separation of propranolol and acebutolol was carried out using a reversed-phase Waters Xterra C_{18} column (2.1 × 100 mm, 3.5 μm). The mobile phase consisted of an 8-min linear gradient from 15:85 to 50:50 0.5% acetic acid/methanol (v/v) followed by a 3-min hold before returning to the initial mobile phase composition at a flow rate of 0.2 mL/min. The retention times of propranolol and the internal standard were 9.2 and 3.6 min, respectively. For the analysis of mannitol, negative ion electrospray and selected ion monitoring were used to record the signal for the deprotonated molecule of mannitol at *m/z* 181 as it eluted from a YMC NH_2 column (2.0 × 150 mm, 5 μM). The mobile phase for the mannitol LC–MS analysis consisted of a 10-min linear gradient from 10:90 to 16:84 water/acetonitrile (v/v) at a flow rate of 0.5 mL/min. Mannitol eluted at 6.6 min under these HPLC conditions. Standard curves were prepared for the LC–MS measurement of mannitol and propranolol in HBSS.

RESULTS

Permeation of the Caco-2 Monolayer

The human intestinal permeability of 8-PN was evaluated using the Caco-2 cell monolayer model system. Under the conditions of these experiments, the rate of 8-PN movement across the monolayer was linear for up to 1 h. The apparent permeability coefficients P_{app} of 8-PN in the apical-to-basolateral (AP → BL) and basolateral-to-apical (BL → AP) directions were $5.2 \pm 0.7 \times 10^{-5}$ and $4.9 \pm 0.5 \times 10^{-5}$ cm/s, respectively. These values are similar to those of drugs such as propranolol and testosterone, which are often used as high-permeability standards.

Metabolism of 8-PN in Caco-2 Monolayers

After 4 h of incubation of 8-PN with human intestinal Caco-2 cells, abundant phase II metabolites were detected on both the apical and basolateral sides of the monolayer. (The relative amounts of these metabolites on each side of the monolayer are discussed below.) The TEER levels after 4 h seemed to drop slightly to 482 ± 35 $\Omega \cdot cm^2$ compared to the initial value of 554 ± 12 $\Omega \cdot cm^2$. Because both values remained well above 300 $\Omega \cdot cm^2$, this indicated that the Caco-2 cell monolayers remained intact.

LC–MS chromatograms of the 8-PN conjugates in aliquots from the apical and basolateral sides of the Caco-2 cell monolayer are shown in Fig. 2. Two glucuronide conjugates of 8-PN (G1 and G2) were detected eluting at 38 and 47 min, respectively. The exact mass measurements of the deprotonated molecules of these metabolites were *m/z* 515.1584 and 515.1587, which were within 5.9 and 6.5 ppm, respectively, of the theoretical molecular formula of $C_{26}H_{27}O_{11}$ for 8-PN monoglucuronide. Treatment of an aliquot of the Caco-2 cell incubation medium with β-glucuronidase resulted in the disappearance of these peaks at 38 and 47 min, which also confirmed that metabolites G1 and G2 were glucuronides. Furthermore, the negative ion electrospray product ion tandem mass spectra of these metabolites (see Fig. 3A) showed a loss of 176 mass units, which is characteristic of glucuronic acid, an ion of *m/z* 175 corresponding to deprotonated dehydrated glucuronic acid, and several low molecular mass fragment ions of *m/z* 113 and 85 corresponding to fragmentation of the glucuronic acid moiety. These data show that the metabolites eluting at 38 and 47 min were glucuronides of 8-PN. However, which peak corresponded to the 7-*O*-glucuronide or the 4′-*O*-glucuronide of 8-PN could not be determined from this information.

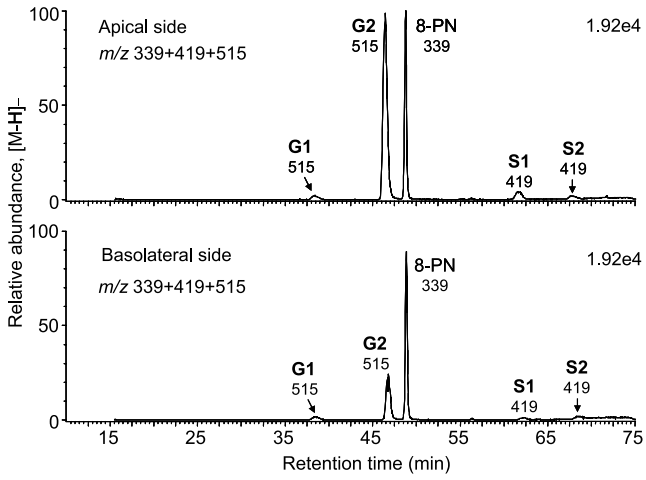

Fig. 2. Computer-reconstructed mass chromatograms of 8-PN (*m/z* 339), 8-PN glucuronides (*m/z* 515), and 8-PN sulfates (*m/z* 419) in aliquots of buffer from the apical and basolateral sides, respectively, of the Caco-2 cell monolayer after incubation with 50 μM 8-PN for 4 h. LC–MS conditions included reversed-phase HPLC separation and negative ion electrospray.

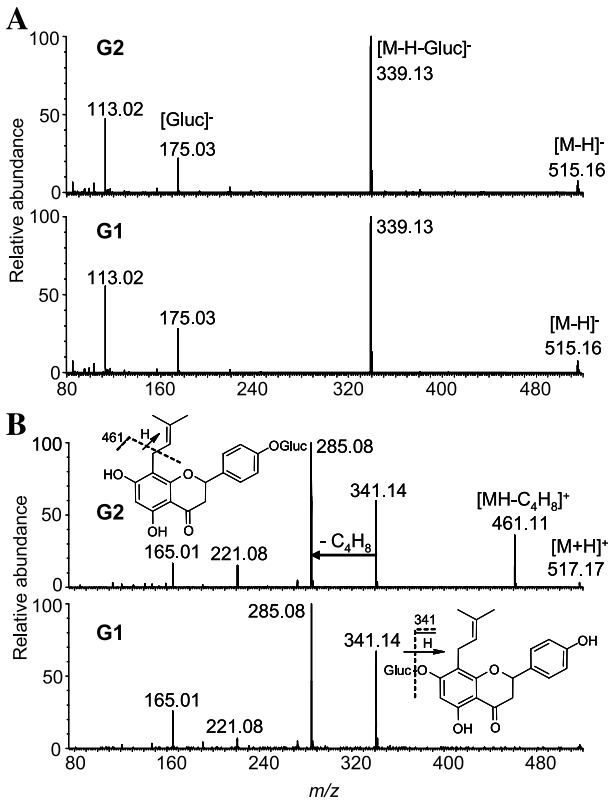

Fig. 3. (A) Negative ion CID product ion mass spectra of glucuronide conjugates of 8-PN. The major fragmentation pathway was elimination of glucuronic acid from the deprotonated molecule. Fragment ions in the low-mass range originated from the glucuronic acid moiety; $[Gluc]^-$ = deprotonated molecule of glucuronic acid. (B) Positive ion CID product ion mass spectra of glucuronide conjugates of 8-PN. Note the fragment ion of *m/z* 461 in the tandem mass spectrum of the 4′-*O* isomer that was formed via a carbocation intermediate stabilized by the free *ortho* hydroxyl group.

Because the negative ion product ion mass spectra (see Fig. 3A) provided no information regarding the position of glucuronidation, positive ion product ion mass spectra of the 8-PN glucuronides were obtained and are shown in Fig. 3B. Although the positive ion product ion tandem mass spectra of 8-PN glucuronides were dominated by the loss of glucuronic acid, a new type of fragment ion was observed at *m/z* 461, which corresponded to the neutral loss of C_4H_8 from the prenyl group of 8-PN glucuronide. The composition of this neutral loss was confirmed by exact mass measurement. Because loss of C_4H_8 produces a carbocation, this fragmentation pathway would be stabilized by an *ortho* hydroxyl group in the C-7 position of 8-PN. Therefore, G2 should correspond to 8-PN 4′-*O*-glucuronide because the ion of *m/z* 461 was more abundant in this positive ion electrospray product ion tandem mass spectrum than in that of G1 (Fig. 3B). Yilmazer *et al.* (8) reported similar fragmentation patterns for glucuronides of xanthohumol.

Metabolite G1 was tentatively identified as the 7-*O*-glucuronide of 8-PN based on Yilmazer *et al.* (8) and the following chemical arguments. Because the 7- and 4′-hydroxyl groups are more acidic than the hydroxyl at the 5-position, these sites might be more susceptible to glucuronidation. In addition, the 5-hydroxyl group would be expected to hydrogen bond with the neighboring carbonyl group to form a six-member chelate, thereby reducing its reactivity toward nucleophilic substitution reactions such as glucuronidation. Similar glucuronidation patterns have been observed for other flavonoids such as chrysin where conjugation occurred only at hydroxyl group in position 7 but not at the hydroxyl group in position 5 (11).

Using a similar approach, the metabolites S1 and S2, eluting at 62 and 67 min, respectively (see Fig. 4), were identified as 8-PN sulfates. The exact masses of the deprotonated molecules of these metabolites were *m/z* 419.0815 and 419.0820, respectively, which were within 3.4 and 4.6 ppm of the theoretical formula of 8-PN monosulfate, $C_{20}H_{19}O_8S$. Treatment of an aliquot of the incubation medium with sulfatase resulted in the disappearance of these peaks (Fig. 4). In addition, the negative ion product ion tandem mass spectra of the deprotonated molecules of these metabolites were dominated by a neutral loss of 80 mass units, which corresponds to the loss of a sulfate moiety (Fig. 4). Unfortunately, informative positive ion electrospray tandem mass spectra of these sulfates could not be obtained due to the lack of formation of abundant protonated molecules. However, the same chemical processes that guided the formation of the 8-PN glucuronides should influence the formation of the

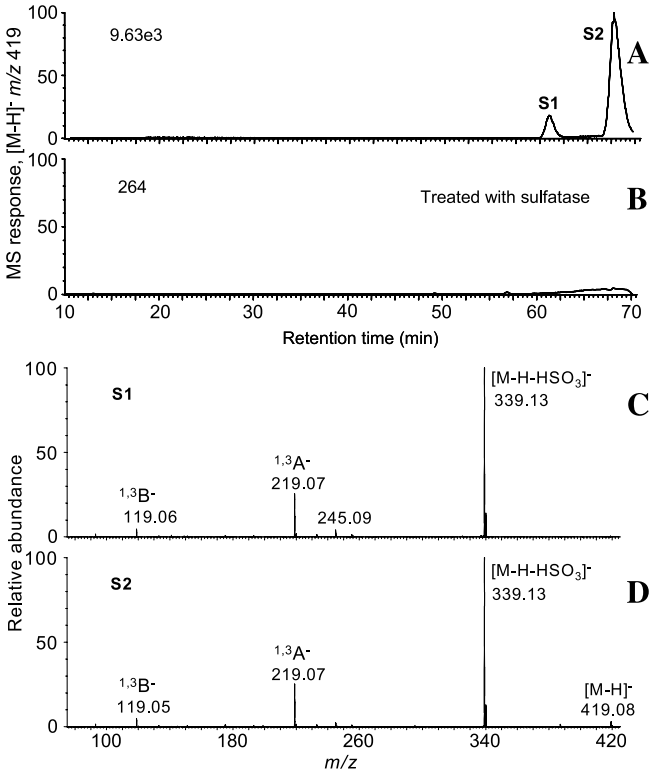

Fig. 4. (A) Computer-reconstructed mass chromatogram of the deprotonated molecules at *m/z* 419 of the 8-PN sulfate conjugates S1 and S2 formed by the Caco-2 cells; (B) mass chromatogram of S1 and S2 after treatment with sulfatase; (C) negative ion CID product ion tandem mass spectrum of S1, a sulfate conjugate of 8-PN that eluted at a retention time of 61 min; and (D) negative ion CID product ion tandem mass spectrum of S2, a sulfate conjugate of 8-PN eluting at 68 min. The major MS–MS fragmentation pathway for both S1 and S2 was elimination of the sulfate group, $[M\text{-}H\text{-}SO_3]^-$, to form the base peak of *m/z* 339. The ions of *m/z* 219 and 119 were retro-Diels–Alder fragment ions of the A ring ($^{1,3}A^-$) and B ring ($^{1,3}B^-$), respectively [see structures in (9)].

8-PN sulfates. Therefore, these two sulfate conjugates were probably 8-PN 4′-sulfate and 8-PN 7-sulfate.

To investigate the possible involvement of an ABC transporter (anionic multidrug-resistance-associated protein, MRP family) on the efflux of 8-PN conjugates, the Caco-2 cell 4-h incubation experiment was repeated in the presence of MK571, which is a well-known inhibitor of ABCC2 (MRP2) (12). Treatment of the Caco-2 cell monolayer with MK571 reduced the apical concentrations of the glucuronides G1 and G2 by 85 ± 3 and 95 ± 4%, respectively. This shows that an ABCC2 (MRP2) pump is probably involved in the efflux of 8-PN glucuronides toward the apical side of the Caco-2 cell monolayer. In contrast to the 8-PN glucuronides, concentrations of 8-PN sulfate conjugates were essentially unchanged after MK571 treatment. The concentration of 8-PN on each side of the Caco-2 cell monolayer was also unaffected by incubation with MK571.

Because no standards of 8-PN glucuronides or sulfates were available, the concentrations of these conjugates were estimated by using UV absorbance and 8-PN as the reference standard. The choice of 8-PN as a standard is supported by the observation that the UV spectra of 8-PN and its metabolites were identical (data not shown). UV measurements were carried out at 294 nm. After incubation of 50 μM 8-PN with a Caco-2 cell monolayer for 4 h, ~54% of the total dose was converted to glucuronides and ~3% to sulfates.

Metabolism of 8-PN by Human Hepatocytes

The total ion chromatogram and computer-reconstructed selected ion chromatograms for the negative ion electrospray LC–MS analysis of an aliquot from the incubation of 50 μM 8-PN with human hepatocytes are shown in Fig. 5. The low intensity of the peak for 8-PN, eluting at 52 min in the total ion chromatogram shown in Fig. 5, indicates that extensive metabolism occurred. Glucuronide conjugates were detected, but not sulfates, which contrasts with the Caco-2 cells that formed abundant sulfate metabolites. In addition, the 7-*O*-glucuronide (G1) of 8-PN was detected as an abundant deprotonated molecule of *m*/*z* 515 at a retention time of 38 min (Fig. 5), whereas the 4′-*O*-glucuronide was not detected. The predominance of G1 formation over G2 in the hepatocyte incubation also differs from the Caco-2 cell incubations in which the 4′-*O*-glucuronide isomer (G2) was more abundant.

As many as six different glucuronide conjugates of 8-PN monooxidation products (G3–G8) were detected as their deprotonated molecules of *m*/*z* 531 (Fig. 5). The two broad peaks eluting between 21 and 26 min in the mass chromatogram of *m*/*z* 531 probably each contained two or more unresolved isomers of 8-PN monooxygenated glucuronides. Two of these conjugates were identified as glucuronides of *cis*- and *trans*-8-PN alcohols (see structures in Fig. 1) based on the fact that after hydrolysis by β-glucuronidase, peaks corresponding to *cis*- and *trans*-8-PN alcohols were enhanced (data not shown). Attempts to identify the specific positions of glucuronidation using mass spectrometry were unsuccessful because in negative ion mode, these glucuronides fragmented almost exclusively to eliminate glucuronic acid without the formation of isomer-specific fragment ions (data not shown). Furthermore, no useful positive ion electrospray

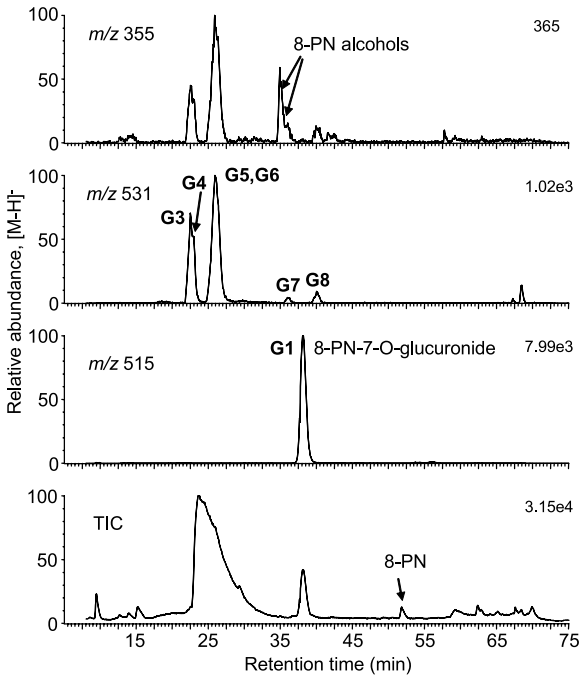

Fig. 5. Computer-reconstructed mass chromatograms and the total ion chromatogram for the negative ion LC–MS analysis of 50 μM 8-PN after incubation with human hepatocytes. Note the intense peak for the 8PN-7-*O*-glucuronide G1 of *m*/*z* 515. No sulfate conjugates were detected. The extent of metabolism is indicated by the peak of low intensity for 8-PN.

MS–MS product ion mass spectra were obtained for these glucuronides. Unambiguous identification of these isomers was also complicated by the fact that glucuronidation introduced an additional chiral center. Therefore, some of the resolved peaks might be glucuronide diastereoisomers.

Minor amounts of *cis*- and *trans*-8-PN alcohols were also detected in the incubation mixture eluting at 35–36 min (see Fig. 5) as the only unconjugated metabolites of 8-PN. The structures of these alcohols were confirmed by comparison with an authentic standard of *trans*-8-PN alcohol and LC–MS–MS exact mass measurements as described elsewhere (9). Following incubation of 8-PN with human hepatocytes, only ~4% was left unmetabolized after 4 h, and the 7-*O*-glucuronide of 8-PN (G1) accounted for ~80% of all metabolites (see Figs. 1 and 5).

Glucuronidation by cDNA-Expressed UDP-Glucuronyl Transferases

To determine which UGT isoforms might be responsible for glucuronidation of 8-PN, we carried out incubations with the cDNA-expressed isoforms of UDP-glucuronyl transferases UGT1A1, UGT1A6, UGT1A8, UGT1A9, UGT1A10, and UGT2B7. UGT1A1, UGT1A6, and UGT2B7 are expressed both in the liver and intestine, and UGT1A9 is expressed by the liver, kidney, and esophagus (13). UGT1A8 and UGT1A10 are expressed specifically in intestinal tissue (14). UGT1A1 was the most active isoform and catalyzed the glucuronidation of ~80% of 8-PN (see Table I) (15). The 7-*O*-glucuronide of 8-PN was the major metabolite followed by the 4′-*O*-glucuronide in a ratio of

Table I. Activities and Regioselectivities of Human Recombinant UDP-Glucuronyl Transferase Isozymes toward 8-PN

Isozyme	Substrate conversion (%)	Ratio of 8-PN 7-*O*-glucuronide to 4′-*O*-glucuronide
UGT1A1	80	98/2
UGT1A6	14	5/95
UGT1A8	23	99/1
UGT1A9	28	96/4
UGT1A10	<1	66/34
UGT2B7	2	33/67

98:2. UGT1A6, UGT1A8, and UGT1A9 displayed moderate activities ranging from 28% conversion for UGT1A9 to 14% for UGT1A6. The two isoforms with the lowest activity toward 8-PN were UGT2B7 and UGT1A10, catalyzing less than 2% conversion of 8-PN. Glucuronidation by various UDP-glucuronyl transferases was also regioselective. UGT1A6 and UGT2B7 preferentially conjugated 8-PN at the 4′-position, whereas the other isoforms preferentially attacked the 7-position.

DISCUSSION

Although *in vitro* assays indicated that 8-PN is only four to five times less estrogenic than estradiol, Milligan *et al.* (6) found that 1000-fold higher concentrations of 8-PN in drinking water were required for efficacy comparable to that of estradiol. These data suggest that the bioavailability of 8-PN is quite low in rats, but no quantitative data are available regarding the absorption of 8-PN in rats or other species. In preparation for clinical studies of hops extracts as alternatives to estrogen replacement therapy, we investigated the intestinal absorption and hepatic metabolism of the estrogenic hops compound 8-PN. To predict whether intestinal absorption, intestinal metabolism, or hepatic metabolism might limit the bioavailability of 8-PN in humans, we used the widely accepted Caco-2 cell model of human intestinal permeability. In addition, we used Caco-2 cells as a model for phase II intestinal conjugation reactions and human hepatocytes as a model for liver metabolism. Our data show that 8-PN exhibits good Caco-2 cell monolayer permeability, with an apparent permeability coefficient similar to well-absorbed drugs such as propranol. Because the P_{app} values for 8-PN were essentially equal in both the apical-to-basolateral and basolateral-to-apical directions, there was no indication of efflux or active transport. Therefore, the mechanism of intestinal absorption of 8-PN is probably passive diffusion.

Although our data predict good intestinal absorption for 8-PN, these data also indicate that extensive phase II conjugation should occur during intestinal absorption. Approximately 50% of the 8-PN added to the incubation medium was converted to phase II conjugates by the human Caco-2 cell monolayers. This suggests that a large fraction of the 8-PN absorbed by the intestine will be conjugated to glucuronide and sulfate metabolites prior to reaching the liver. Although the Caco-2 cell model is recognized more as a model of human intestinal absorption than of phase II intestinal metabolism, there are many examples of conjugation reactions of xenobiotics by Caco-2 cells in the literature. For example, Caco-2 cell monolayers have been reported to form conjugates of dietary phenolic compounds such as chrysin (16), genistein, apigenin (17), and (−)epicatechin (18). In addition, several pharmaceutical compounds have been shown to be metabolized by Caco-2 cells including L-α-methyldopa (19), apomorphine, dobutamine (20), and various nonsteroidal anti-inflammatory drugs (21). Furthermore, based on enzyme assays, Prueksaritanont *et al.* reported that Caco-2 cells express all conjugating activities except for the sulfation of acetaminophen (22).

During incubation of 8-PN with Caco-2 cells, the phase II conjugates of 8-PN were concentrated on the apical side of the cell monolayer whether 8-PN was added initially to the apical side or to the basolateral side. These observations suggested the existence of an efflux mechanism that pumps these polar metabolites out of the cell in the apical direction. The protein responsible for the efflux of the 8-PN glucuronides G1 and G2 was identified as ABCC2 (MRP2) based on inhibition by MK571. It should be noted that no Caco-2 cytotoxicity was noted due to incubation with MK571 because the TEER values were unchanged compared to incubations that did not contain MK571. Furthermore, the concentrations of the sulfate conjugates on the apical and basolateral sides of the monolayer were unaffected by treatment with MK571. Previous studies on the metabolism of xenobiotics by Caco-2 cells determined the existence of a family of efflux proteins known as MRP (ATP binding cassette) that eliminates anionic metabolites such as glucuronides and sulfates (23). One member of the family, ABCC2 (MRP2), is localized exclusively to the apical domain of polarized cells such as intestinal epithelial cells (24). These characteristics of MRP are consistent with our results in which efflux of 8-PN glucuronides to the apical side of the Caco-2 cells was observed by ABCC2 (MRP2). It is interesting to note that the ABCC2 (MRP2) inhibitor MK571 did not affect the efflux of sulfates. This finding is consistent with observations of others that glucuronides and sulfates are substrates for separate transporters (23).

The metabolic profiles of 8-PN obtained using human hepatocytes and the Caco-2 preparations were quite different. Whereas Caco-2 cells formed both glucuronides and sulfates, only glucuronides of 8-PN were observed in hepatocyte incubations. Furthermore, Caco-2 cells formed predominantly 4′-*O*-glucuronide and some 7-*O*-glucuronide, whereas hepatocytes formed almost exclusively the 7-*O*-glucuronide of 8-PN. These data indicate that there is differential expression between the human hepatocytes and Caco-2 cells of the UGT and sulfotransferase isoforms responsible for conjugation of 8-PN.

The results of the incubations with human hepatocytes suggest that 8-PN will exhibit high first-pass hepatic metabolism because only 4% of 8-PN remained unmetabolized after a 4-h incubation. The 7-*O*-glucuronide of 8-PN accounted for ~80% of the original dose, with the remainder being glucuronides of phase I metabolites, small amounts of unconjugated phase I products, and 4% unchanged 8-PN.

Consistent with our previous studies of the metabolism of 8-PN by human liver microsomes, the 8-PN alcohols were the most abundant phase I metabolites in the hepatocyte incubation (9). Like 8-PN, only a small fraction of these 8-PN alcohols were detected in their unconjugated form, which indicated a high efficiency of glucuronidation of these compounds. Because these *in vitro* experiments predict that extensive hepatic as well as intestinal metabolism of 8-PN should occur *in vivo*, only a minor fraction of orally administered 8-PN would be expected to reach the systemic circulation unchanged. This might explain the low *in vivo* efficacy of 8-PN in studies by Milligan *et al.* (6).

Our experiments with cDNA-expressed UGT isoforms provided additional insights into the metabolism of 8-PN. Among the isoforms tested, UGT1A1 showed the highest activity toward 8-PN and is probably primarily responsible for conjugation of 8-PN *in vivo*. In the liver, UGT1A1 is the primary enzyme responsible for conjugation of bilirubin and several clinically important drugs including irinotecan, buprenorphine, and ethinylestradiol. Interestingly, estradiol is also a substrate for UGT1A1. Therefore, the UGT1A1 active site might be highly complementary to the estrogen receptor ligand binding site. It would be interesting to determine whether other estrogens from botanical sources are metabolized by this isoform.

Another important characteristic of UGT1A1 is genetic variation of this isoform among individuals. Fisher *et al.* (25) examined glucuronidation rates for some UGT1A1-selective substrates in a bank of 20 livers and found that the rates of metabolism between individuals varied as much as 30-fold. Severely decreased expression of the UGT1A1 isoform, known as Gilbert's syndrome and characterized by asymptomatic unconjugated hyperbilirubinemia, occurs among 2–19% of various populations (26). These patients typically exhibit reduced clearance of the drugs that are primarily eliminated by glucuronidation. Our data suggest that the bioavailability of 8-PN would be much higher in individuals whose expression of UGT1A1 is impaired.

UGT1A1 has also been found in intestinal tissues (15). Interestingly, this isoform was not detected in untreated Caco-2 cells but was found to be significantly induced by dietary flavonoids such as chrysin and quercetin (27,28). In addition, quercetin was found to induce UGT1A6 and the ABCC2 (MRP2) transporter (24). Because quercetin and chrysin are abundant in the human diet, they would probably contribute to the up-regulation of UGT1A1 and UGT1A6 and reduce the bioavailability of 8-PN both via increased intestinal and hepatic glucuronidation. Other UGT-inducing compounds might be present in hops extracts as well. It is unknown at this time whether 8-PN itself induces any UGT isozymes.

UGT1A9 also exhibited moderate activity toward 8-PN. In addition to liver, this isoform is expressed in the kidney and esophagus. Expression in kidney is even more prevalent than in the liver; thus, this isoform might contribute significantly to the extrahepatic clearance of 8-PN. It is interesting to note that naringenin, a close analog of 8-PN, has also been shown to be a good substrate for UGT1A9 (14). Among intestine-specific isoforms, only UGT1A8 showed activity toward 8-PN and was probably responsible primarily for the formation of 7-*O*-glucuronide in Caco-2 cells.

Overall, these data indicate that the formation of 4′-*O*-glucuronide in Caco-2 cells was probably catalyzed primarily by UGT1A6 and that UGT1A1 is another important isozyme responsible for the formation of most of the 8-PN 7-*O*-glucuronide in human hepatocytes. Because the UGT1A1 isoform is not expressed in untreated Caco-2 cells (15), formation of 7-*O*-glucuronide by this cell line was probably catalyzed by UGT1A8 and possibly UGT1A9, although expression of this isoform in Caco-2 cells is largely unknown. The relative contributions of other isoforms of UDP-glucuronyl transferases to the glucuronidation of 8-PN in Caco-2 cells are unknown at this time.

Although caution must be used when extrapolating Caco-2 data to humans, there are examples of such *in vitro* predictions that have been validated *in vivo*. In one example, studies of chrysin using Caco-2 and HepG2 cells predicted low and variable bioavailability due to extensive metabolism. In a subsequent phase I clinical study, Walle *et al.* (29) found that chrysin showed variable but poor bioavailability ranging from 0.003 to 0.8% of the administered dose. Walle *et al.* (29) concluded that aromatase inhibition by chrysin was negligible because pharmacologically relevant concentrations could not be achieved following oral administration. Similarly, we predict poor oral bioavailability and low estrogenicity *in vivo* for 8-PN due to extensive intestinal and hepatic metabolism catalyzed primarily by UGT1A1. In general, UGT1A1-mediated metabolic clearance is considered an undesirable characteristic of a potential drug candidate; as a result, UGT1A1 has been described as the "CYPD6 of phase II metabolism" (25). The role of inducible UGT1A1 in the conjugation of 8-PN might explain the anecdotal human reports of the estrogenicity of hops and the weak estrogenicity of hops in rats (6). Phenotyping women for UGT1A1 activity in future clinical trials of hops estrogenicity might help explain response differences among the population. In addition, future studies should assess the potential for enterohepatic recirculation of 8-PN because this might be a mechanism for increasing serum levels of 8-PN during chronic administration. If enterohepatic recirculation occurs in humans, then pharmacologically effective concentrations of 8-PN might be achieved, which would need to be only in the nanomolar range.

Because dietary exposure to 8-PN occurs primarily through the consumption of beer, this should have little impact on human health given the low oral bioavailability of 8-PN predicted by our studies and the small amounts usually found in beer (30). Of greater concern would be the consumption of dietary supplements containing hops extracts. Given the high estrogenicity of 8-PN *in vitro*, hops dietary supplements should be used in moderation until the human bioavailability and *in vivo* pharmacokinetics of 8-PN are fully resolved. Finally, the data presented in this paper should be useful for the design of future clinical trials of hops dietary supplements for safety and efficacy.

ACKNOWLEDGMENTS

We thank Jim Boyd and Yakima Chief, Inc. (Sunnyside, WA, USA) for providing plant material. This research was supported by grant P50AT00155 provided to the UIC/NIH Center for Botanical Dietary Supplements Research by the

Office of Dietary Supplements, the National Institute of General Medical Sciences, the Office for Research on Women's Health, and the National Center for Complementary and Alternative Medicine. The content is the responsibility of the authors and does not necessarily represent the official views of the sponsors.

REFERENCES

1. S. R. Milligan, J. C. Kalita, A. Heyerick, H. Rong, L. De Cooman, and D. De Keukeleire. Identification of a potent phytoestrogen in hops (*Humulus lupulus* L.) and beer. *J. Clin. Endocrinol. Metab.* **83**:2249–2252 (1999).
2. N. G. Coldham and M. J. Sauer. Identification, quantitation and biological activity of phytoestrogens in a dietary supplement for breast enhancement. *Food Chem. Toxicol.* **39**:1211–1224 (2001).
3. J. F. Stevens, M. Ivancic, V. L. Hsu, and M. L. Deinzer. Prenylflavonoids from *Humulus lupulus*. *Phytochemistry* **44**:1575–1585 (1997).
4. M. Kitaoka, H. Kadokawa, M. Sugano, K. Ichikawa, M. Taki, S. Takaishi, Y. Iijima, S. Tsutsumi, M. Boriboon, and T. Akiyama. Prenylflavonoids: a new class of non-steroidal phytoestrogen (part 1). Isolation of 8-isopentenylnaringenin and an initial study on its structure–activity relationship. *Planta Med.* **64**:511–515 (1998).
5. O. Zierau, S. Gester, P. Schwab, P. Metz, S. Kolba, M. Wulf, and G. Vollmer. Estrogenic activity of the phytoestrogens naringenin, 6-(1,1-dimethylallyl)naringenin and 8-prenylnaringenin. *Planta Med.* **68**:449–451 (2002).
6. S. Milligan, J. Kalita, V. Pocock, L. Heyerick, L. De Cooman, H. Rong, and D. De Keukeleire. Oestrogenic activity of the hop phyto-estrogen, 8-prenylnaringenin. *Reproduction* **123**:235–242 (2002).
7. M. Yilmazer, J. F. Stevens, M. L. Deinzer, and D. R. Buhler. *In vitro* biotransformation of xanthohumol, a flavonoid from hops (*Humulus lupulus*) by rat liver microsomes. *Drug Metab. Dispos.* **29**:223–231 (2001).
8. M. Yilmazer, J. F. Stevens, and D. R. Buhler. *In vitro* glucuronidation of xanthohumol, a flavonoid in hop and beer, by rat and human liver microsomes. *FEBS Lett.* **491**:252–256 (2001).
9. D. Nikolic, Y. Li, L. R. Chadwick, S. Grubjesic, P. Schwab, P. Metz, and R. B. van Breemen. Metabolism of 8-prenylnaringenin, a potent phytoestrogen from hops (*Humulus lupulus*) by human liver microsomes. *Drug Metab. Dispos.* **32**:272–279 (2004).
10. M. B. Fisher, K. Campanale, B. L. Ackermann, M. VandenBranden, and S. A. Wrighton. *In vitro* glucuronidation using human liver microsomes and the pore-forming peptide alamethicin. *Drug Metab. Dispos.* **28**:560–566 (2000).
11. A. Galijatovic, Y. Otake, U. K. Walle, and T. Walle. Extensive metabolism of the flavonoid chrysin by human Caco-2 and Hep G2 cells. *Xenobiotica* **29**:1241–1256 (1999).
12. I. Leier, G. Jedlitschky, U. Buchholz, S. P. Cole, R. G. Deeley, and D. Keppler. The *MRP* gene encodes an ATP-dependent export pump for leukotriene C_4 and structurally related conjugates. *J. Biol. Chem.* **269**:27807–27810 (1994).
13. C. P. Strassburg, A. Strassburg, N. Nguyen, Q. LiL, M. P. Manns, and R. H. Tukey. Regulation and function of family 1 and family 2 UDP-glucuronosyltransferase genes (UGT1A, UGT2B) in human oesophagus. *Biochem. J.* **338**:489–498 (1999).
14. Z. Cheng, A. Radominska-Pandya, and T. R. Tephly. Studies on the substrate specificity of human intestinal UDP-glucuronosyltransferases 1A8 and 1A10. *Drug Metab. Dispos.* **27**:1165–1170 (1999).
15. M. F. Paine and M. B. Fisher. Immunochemical identification of UGT isoforms in human small bowel and in Caco-2 cell monolayers. *Biochem. Biophys. Res. Commun.* **273**:1053–1057 (2000).
16. U. K. Walle, A. Galijatovic, and T. Walle. Transport of the flavonoid chrysin and its conjugated metabolites by the human intestinal cell line Caco-2. *Biochem. Pharmacol.* **58**:431–438 (1999).
17. Y. Liu and M. Hu. Absorption and metabolism of flavonoids in the Caco-2 cell culture model and a perfused rat intestinal model. *Drug Metab. Dispos.* **30**:370–377 (2002).
18. J. Vaidyanathan and T. Walle. Transport and metabolism of the tea flavonoids (−)-epicatechin by the human intestinal cell line Caco-2. *Pharm. Res.* **18**:1420–1425 (2001).
19. P. J. Chikhale and R. T. Borchardt. Metabolism of L-α-methyldopa in cultured human intestinal epithelial (CACO-2) cell monolayers. Comparison with metabolism *in vivo*. *Drug Metab. Dispos.* **22**:592–600 (1994).
20. L. Antonio, J. Xu, J. M. Little, B. Burchell, J. Magdalou, and A. Radominska-Pandya. Glucuronidation of catechols by human hepatic, gastric, and intestinal microsomal UDP-glucuronosyltransferases (UGT) and recombinant UGT1A6, UGT1A9, and UGT2B7. *Arch. Biochem. Biophys.* **411**:251–261 (2003).
21. N. Sabolovic, J. Magdalou, P. Netter, and A. Abid. Nonsteroidal anti-inflammatory drugs and phenols glucuronidation in Caco-2 cells: identification of the UDP-glucuronosyltransferases UGT1A6, 1A3 and 2B7. *Life Sci.* **67**:185–196 (2000).
22. T. Prueksaritanont, L. M. Gorham, J. H. Hochman, L. O. Tran, and K. P. Vyas. Comparative studies of drug-metabolizing enzymes in dog, monkey, and human small intestines, and in Caco-2 cells. *Drug Metab. Dispos.* **24**:634–642 (1996).
23. J. König, A. T. Nies, Y. Cui, I. Leirer, and D. Keppler. Conjugate export pumps of the multidrug resistance protein (MRP) family: localization, substrate specificity, and MRP2-mediated drug resistance. *Biochim. Biophys. Acta* **1461**:377–394 (1999).
24. K. W. Bock, T. Eckle, M. Ouzzine, and S. F. Gigleux. Coordinate induction by antioxidants of UDP-glucuronosyltransferase UGT1A6 and the apical conjugate export pump MRP2 (multidrug resistance protein 2) in Caco-2 cells. *Biochem. Pharmacol.* **59**:467–470 (2000).
25. M. B. Fisher, M. F. Paine, T. J. Strelevitz, and S. A. Wrighton. The role of hepatic and extrahepatic UDP-glucuronosyltransferases in human drug metabolism. *Drug Metab. Rev.* **33**:273–297 (2001).
26. D. J. Clarke, N. Moghrabi, G. Monaghan, A. Cassidy, M. Boxer, R. Hume, and B. Burchell. Genetic defects of the UDP-glucuronosyltransferase-1 (UGT1) gene that cause familial non-hemolytic unconjugated hyperbilirubinemias. *Clin. Chim. Acta* **266**:63–74 (1997).
27. A. Galijatovic, Y. Otake, U. K. Walle, and T. Walle. Induction of UDP-glucuronosyltransferase UGT1A1 by the flavonoid chrysin in Caco-2 cells-potential role in carcinogen bioinactivation. *Pharm. Res.* **18**:374–379 (2001).
28. A. Galijatovic, U. K. Walle, and T. Walle. Induction of UDP-glucuronosyltransferase by the flavonoids chrysin and quercetin in Caco-2 cells. *Pharm. Res.* **17**:21–26 (2000).
29. T. Walle, Y. Otake, J. A. Brubaker, U. K. Walle, and P. V. Haluska. Disposition and metabolism of the flavonoid chrysin in normal volunteers. *Br. J. Clin. Pharmacol.* **51**:143–146 (2001).
30. J. Tekel, D. De Keukeleire, H. Rong, E. Daeseleire, and C. Van Peteghem. Determination of the hop-derived phytoestrogen, 8-prenylnaringenin, in beer by gas chromatography/mass spectrometry. *J. Agric. Food Chem.* **47**:5059–5063 (1999).